Electronic Supplementary Information (ESI)

Ultrathin Nickel Hydroxide Nanosheets with Porous Structure for Efficient Electrocatalytic Urea Oxidation

Wenlong Yang, Xianpeng Yang, Bijun Li, Jiehua Lin, Hongtao Gao, Changmin Hou and Xiliang Luo**

Dr. W. L. Yang, X. P. Yang, B. J. Li, Prof. J. H. Lin, Prof. H. T. Gao, C. M. Hou, Prof. X. L. Luo

Key Laboratory of Optic-electric Sensing and Analytical Chemistry for Life Science, MOE,

Key Laboratory of Analytical Chemistry for Life Science in Universities of Shandong,

College of Chemistry and Molecular Engineering,

Qingdao University of Science and Technology,

Qingdao 266042, P. R. China

E-mail: xiliangluo@qust.edu.cn; gaohtao@qust.edu.cn

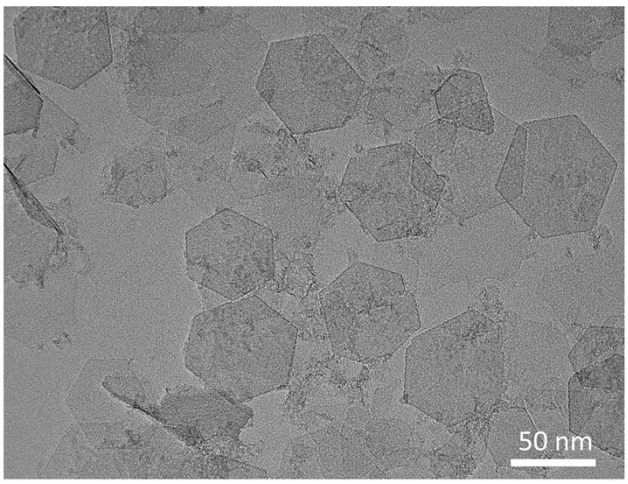

Fig. S1. TEM image of the as-obtained porous $Ni(OH)_2$ nanosheets, revealing their porous structures and ultrathinness feature.

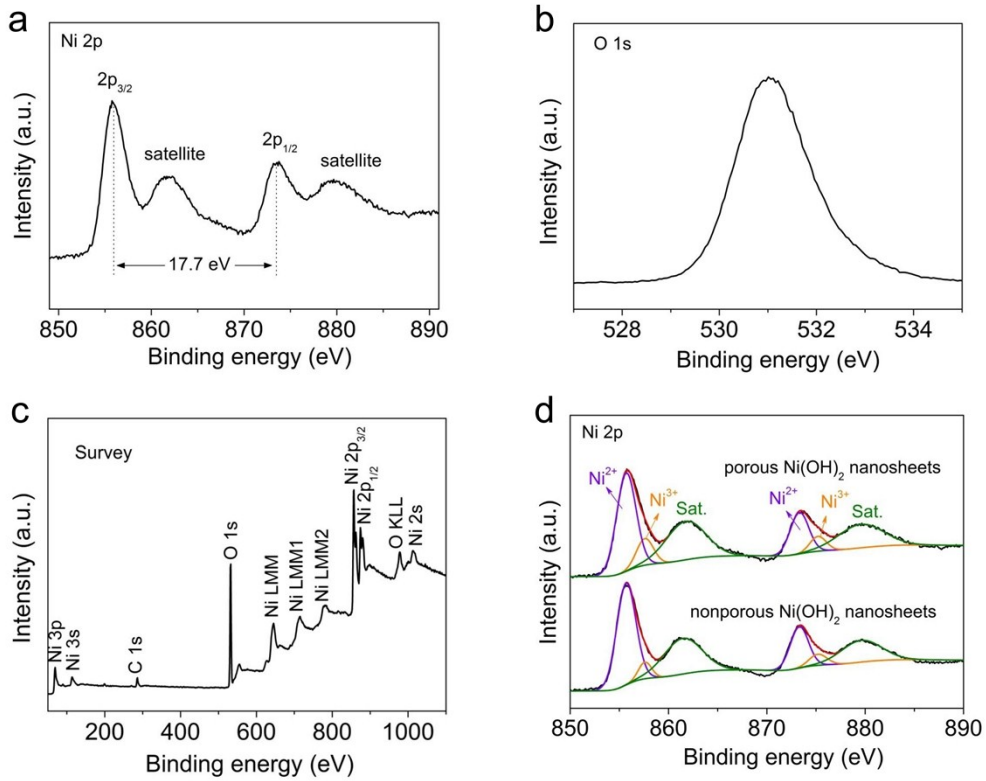

Fig. S2. (a) Ni 2p spectra, (b) O 1s spectra and (c) XPS survey spectra of the as-obtained porous $Ni(OH)_2$ nanosheets. (d) Comparison of the Ni 2p spectra of porous and nonporous $Ni(OH)_2$ nanosheets.

The detailed elemental composition and the oxidation state of the as-obtained porous $Ni(OH)_2$ nanosheets are further investigated by X-ray photoelectron spectroscopy (XPS) measurement, which is presented in Fig. S2. As shown in Fig. S2a, a pair of prominent peaks at the binding energies of 855.8 eV and 873.5 eV can be assigned to the Ni $2p_{3/2}$ and $2p_{1/2}$, respectively, and the other two peaks are their corresponding satellite peaks, which indicates the crystal phase of $Ni(OH)_2$.[1] As shown in Fig. S2d, the high-resolution Ni 2p spectra of the porous β-$Ni(OH)_2$ nanosheets was deconvoluted. Two characteristic peaks at 855.7 and 873.4 eV are assigned to the $2p_{3/2}$ and $2p_{1/2}$ signals of Ni^{2+}, while the peaks at 857.6 and 875.2 eV can be assigned to signals of Ni^{3+}.[4]

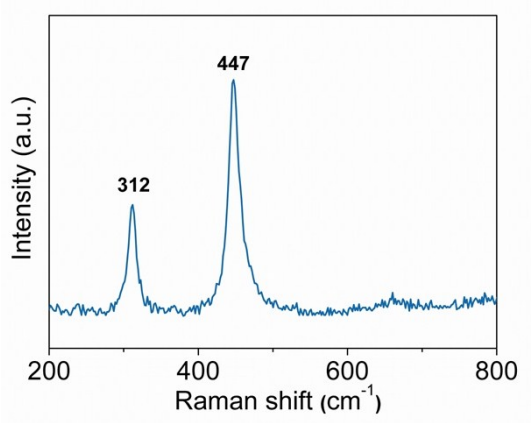

Fig. S3. Raman spectra of porous $Ni(OH)_2$ nanosheets.

Raman spectra shown in Fig. S3 provides an additional insight into the chemical composition of the obtained porous $Ni(OH)_2$ nanosheets. In detal, two Raman peaks center at 312 and 447 cm^{-1} can be be observed, which can be ascribed to the $E_u(T)$ and $A_{2u}(T)$ lattice vibrations of hexagonal $Ni(OH)_2$, respectively.[2]

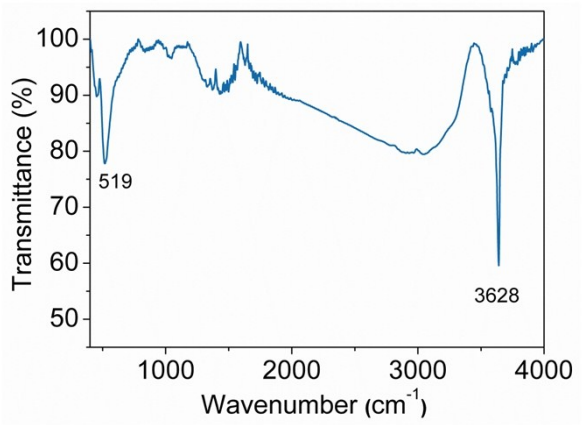

Fig. S4. Fourier Transform Infrared Spectroscopy (FTIR) spectrum of porous $Ni(OH)_2$ nanosheets.

As shown in Fig. S3. The prominent peaks at 3628 cm^{-1} is assigned to the stretching vibrational mode of hydroxyl groups in the brucite-like sheet structure. While the band at 519 cm^{-1} is attributed to Ni-O stretching and Ni-OH bending vibration in the brucite-like octahedral sheet, which is the birthmark for the β-$Ni(OH)_2$. In addition, the broad band at around 3000 cm^{-1} is to ascribed the bending vibrations of absorbed water molecules.[3]

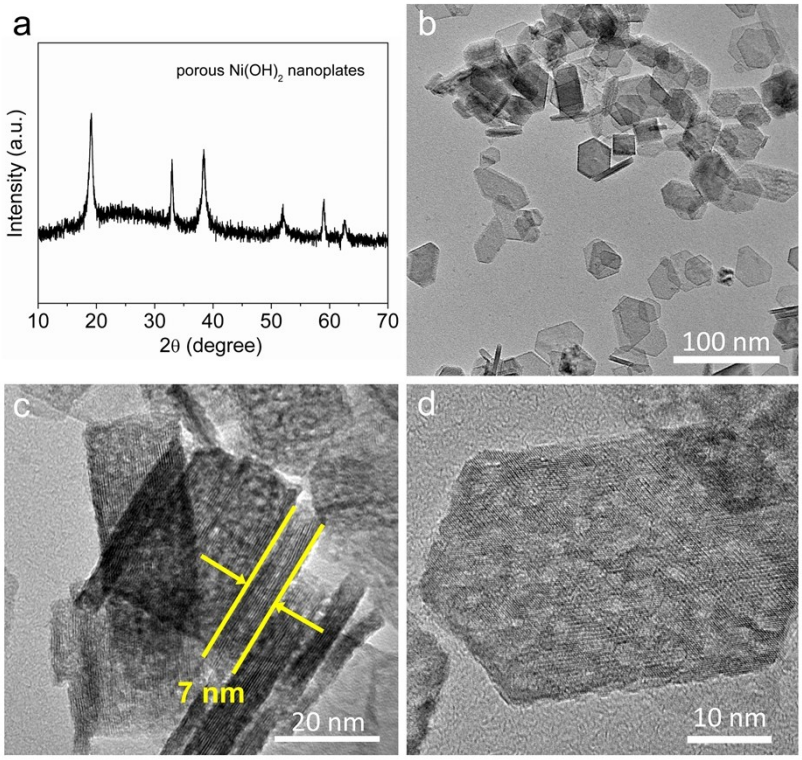

Fig. S5. (a) XRD pattern, (b-d) TEM images of the prepared porous $Ni(OH)_2$ nanoplates. From which the hexagonal plate-like morphology and abundant pores as well as the thickness of about 7 nm can be identified.

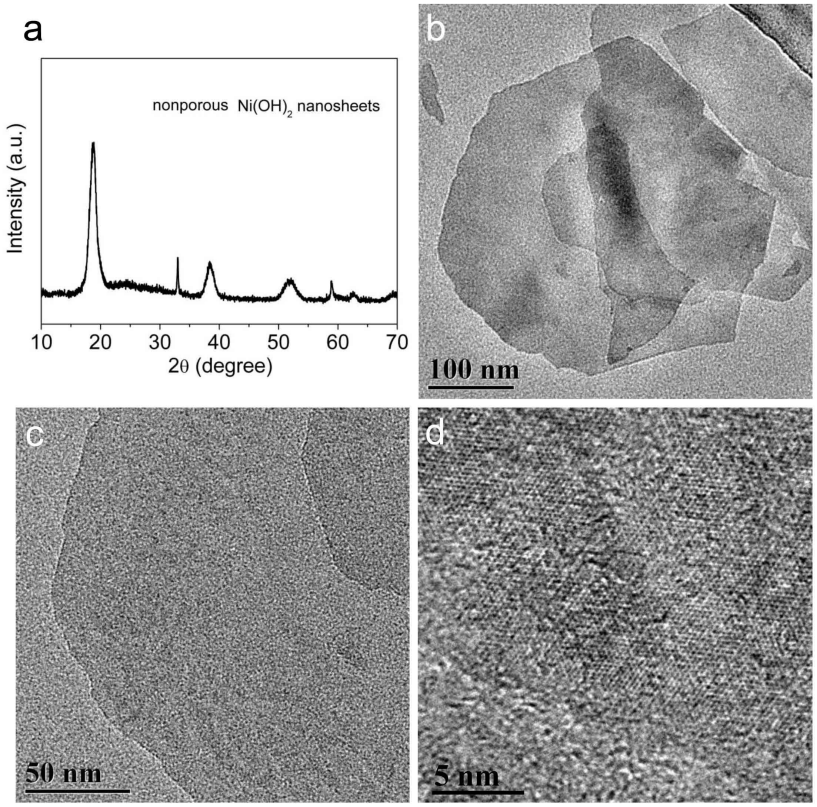

Fig. S6. (a) XRD pattern, (b-d) TEM images of the prepared nonporous $Ni(OH)_2$ nanosheets. From which the ultrathin thickness and the extremely low amount of pores can be observed.

The XRD pattern demonstrates the pure crystalline phase of β-$Ni(OH)_2$. And the TEM and HRTEM images of obtained β-$Ni(OH)_2$ confirm its sheet-like morphology and ultrathin thickness, from which no obvious pores can be identified, indicating the successful fabrication of nonporous ultrathin $Ni(OH)_2$ nanosheets.

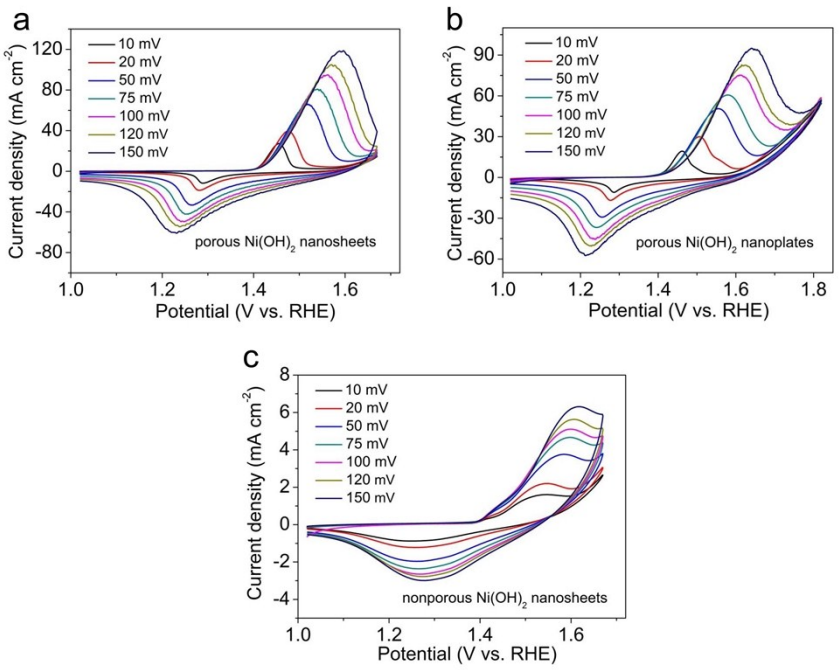

Fig. S7. CV curves of (a) porous $Ni(OH)_2$ nanosheets, (b) porous $Ni(OH)_2$ nanoplates and (c) nonporous $Ni(OH)_2$ nanosheets in 1 M KOH solution at potential sweep rates of 10, 20, 50, 75, 100, 120 and 150 mV/s.

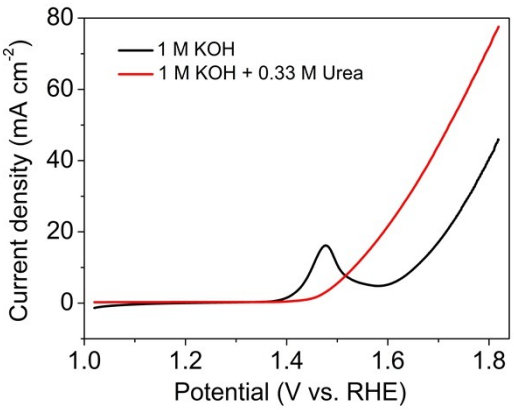

Fig. S8. Linear sweep voltammetry curves of porous $Ni(OH)_2$ nanoplates measured in 1 M KOH solution with and without 0.33 M urea at a scan rate of 20 mV S^{-1}.

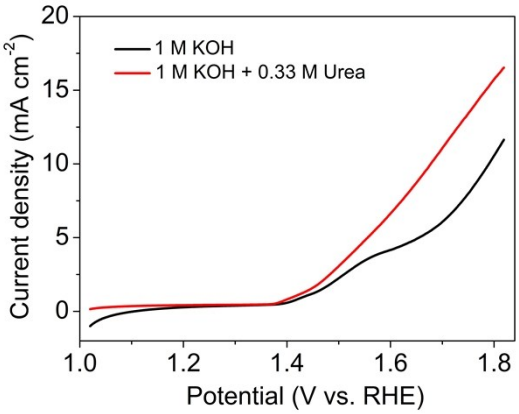

Fig. S9. Linear sweep voltammetry curves of nonporous $Ni(OH)_2$ nanosheets measured in 1 M KOH solution with and without 0.33 M urea at a scan rate of 20 mV S^{-1}.

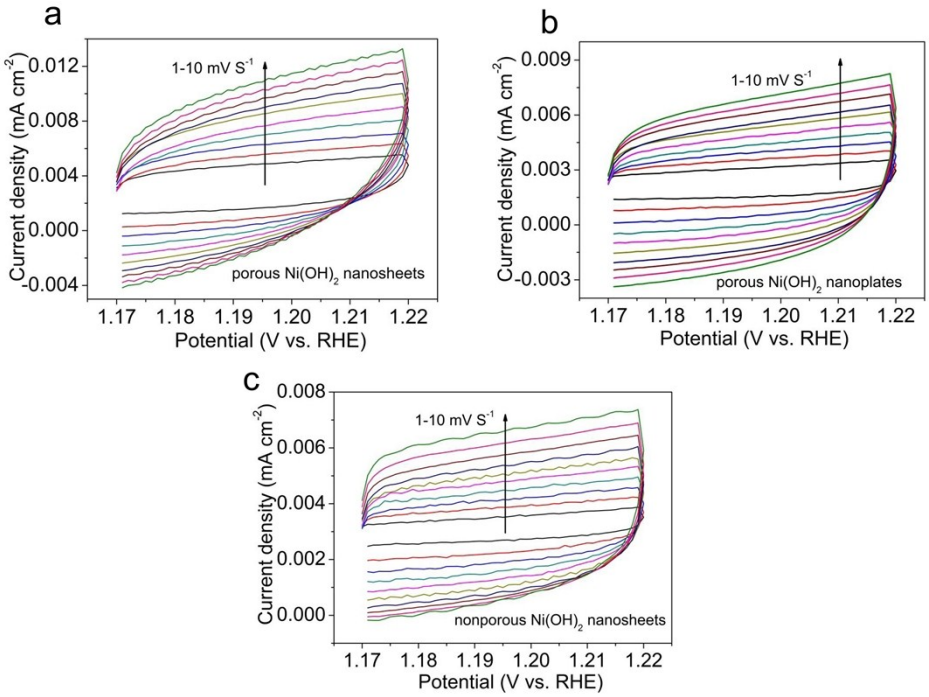

Fig. S10. Cyclic voltammetry curves of (a) porous $Ni(OH)_2$ nanosheets, (b) porous $Ni(OH)_2$ nanoplates, and (c) nonporous $Ni(OH)_2$ nanosheets measured in 1M KOH solution at scan rates from 1 to 10 mVs^{-1}.

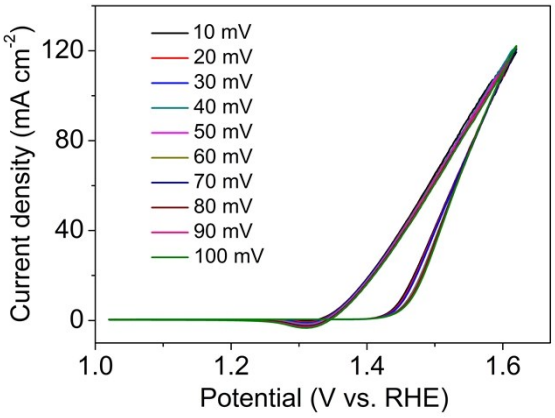

Fig. S11. Cyclic voltammetry curves of porous $Ni(OH)_2$ nanosheets at different scan rates.

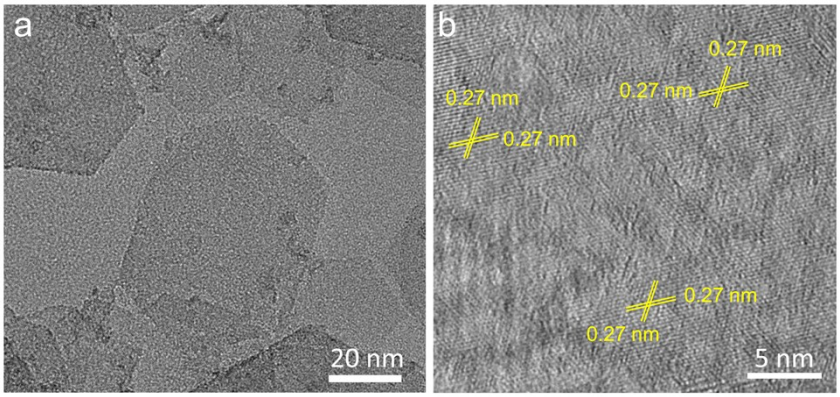

Fig. S12. (a) TEM image and (d) HRTEM image of $Ni(OH)_2$ nanosheets after 3 minutes of microwave irradiation.

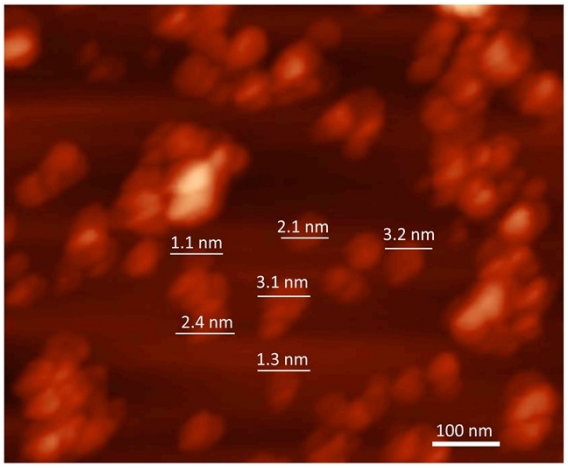

Fig. S13. AFM image of porous $Ni(OH)_2$ nanosheets. From which obvious stacking of individual nanosheets rather than thick sheets can be observed, revealing the ultrathin feature of the obtained nanosheets.

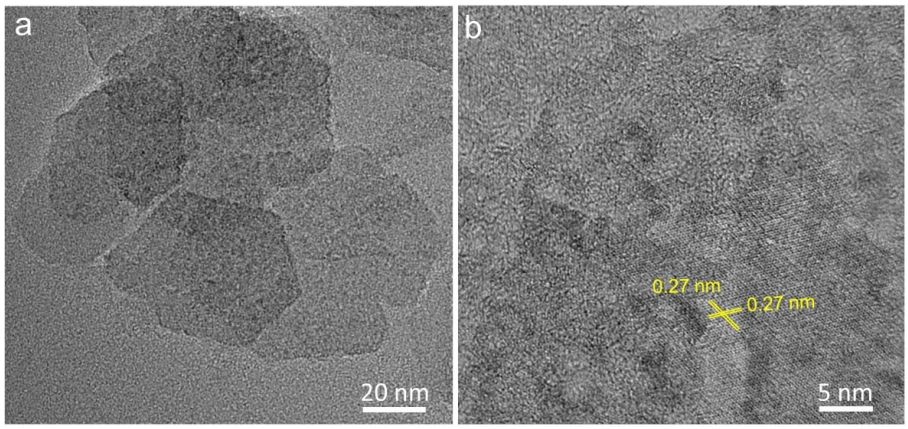

Fig. S14. (a) TEM image and (b) HRTEM image of porous $Ni(OH)_2$ nanosheets after the chronoamperometric test in 1 M KOH solution containing 0.33 M urea.

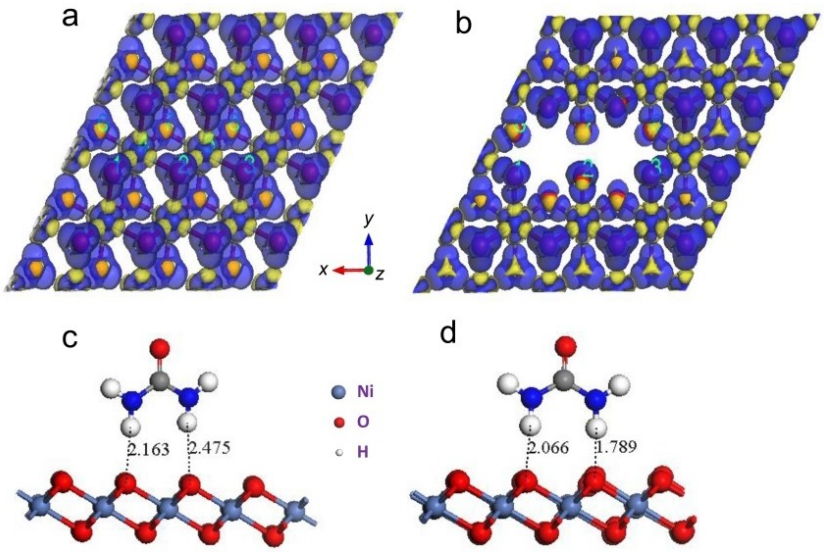

Fig. S15. The differential charge densities of (a) β-$Ni(OH)_2$ slab and (b) β-$Ni(OH)_2$ slab with large V_{Ni2}. The distances between two H atoms form urea and (c) β-$Ni(OH)_2$ slab and (d) β-$Ni(OH)_2$ slab with large V_{Ni2}.

Table S1. Comparison of the electrocatalytic UOR activity between the porous $Ni(OH)_2$ nanosheets and other recently reported catalysts.

Catalyst	Current density (mA cm^{-2})	Potential /V vs. RHE	Substrate	Catalyst loading (mg cm^{-2})	Electrolyte	Scan rate (mV s^{-1})	Reference
Porous $Ni(OH)_2$ nanosheets	109.7	1.6	Glassy carbon	0.285	1 M KOH, 0.33 M urea	20	This work
Ni-Cr	~90	1.6	Glassy carbon	0.05	1 M KOH, 0.33 M urea	10	ChemCatChem, 2017, 9, 3374
Ni-Co	~20	1.6	Glassy carbon	0.848	1 M KOH, 0.33 M urea	50	Sci. Rep., 2014, 4, 5863
Metallic $Ni(OH)_2$	~36	1.52	Glassy carbon	0.535	1 M KOH, 0.33 M urea	50	Angew. Chem. Int. Ed., 2016, 55, 12465
Ni-MOF	~41	1.6	Glassy carbon	0.191	1 M KOH, 0.33 M urea	10	Chem. Commun., 2017, 53, 10906
Bimetallic NiCoP nanosheets	~100	1.6	Carbon cloth	--	1 M KOH, 0.33 M urea	2	ChemistrySelect, 2017, 2, 10285
Pristine Ni MOF	~90	1.6	Glassy carbon	0.48	1 M KOH, 1 M urea	5	ChemElectroChem, 2018, 5, 2795
Ni_2P-C	~70	1.55	Glassy carbon	0.38	1 M KOH, 0.33 M urea	10	ChemElectroChem, 2018, 5, 659
$Ni(OH)_2$/carbon fiber cloth	~100	1.6	Carbon cloth	0.18	1 M KOH, 0.5 M urea	5	Chem. Commun., 2017, 53, 10711
$Ni_{1.5}Mn_{1.5}O_4$	~7	1.55	Glassy carbon	0.05	1 M KOH, 0.33 M urea	10	ACS Appl. Mater. Interfaces, 2016, 8, 12176
V_{Ni}-rich α-$Ni(OH)_2$	~110	1.6	Glassy carbon	0.142	1 M KOH, 0.33 M urea	50	ACS Energy Lett., 2018, 3, 1373
$Ni(OH)_2$/PPy/GO	~12	1.6	Glassy carbon	0.072	1 M KOH, 0.5 M urea	10	ACS Sustainable Chem. Eng., 2018, 6, 15570
20% Pt/C	~5	1.6	Glassy carbon	0.191	1 M KOH, 0.33 M urea	10	Chem. Commun., 2017, 53, 10906

References

[1] K. Xu, H. Ding, K. C. Jia, C. Z. Wu, X. Yi, *Angewandte Chemie* **2016**, *55*, 1710.

[2] J. Yan, W. Sun, T. Wei, Q. Zhang, Z. J. Fan, F. Wei, *J. Mater. Chem.* **2012**, *22*, 11494.

[3] S. Sarkar, M. Pradhan, A. K. Sinha, M. Basu, Y. Negishi, T. Pal, *Inorg. Chem.* **2010**, *49*, 8813.

[4] Q. He, Y. Y. Wan, H. L. Jiang, Z. W. Pan, C. Q. Wu, M. Wang, X. J. Wu, B. J. Ye, P. M. Ajayan, L. Song, *ACS Energy Lett.* **2018**, *3*, 1373.